Stair Ascent Phase-Variable Control of a Powered Knee-Ankle Prosthesis

Ross J. Cortino, Edgar Bolívar-Nieto, T. Kevin Best, and Robert D. Gregg

***Abstract*— Passive prostheses cannot provide the net positive work required at the knee and ankle for step-over stair ascent. Powered prostheses can provide this net positive work, but user synchronization of joint motion and power input are critical to enabling natural stair ascent gaits. In this work, we build on previous phase variable-based control methods for walking and propose a stair ascent controller driven by the motion of the user's residual thigh. We use reference kinematics from an able-bodied dataset to produce knee and ankle joint trajectories parameterized by gait phase. We redefine the gait cycle to begin at the point of maximum hip flexion instead of heel strike to improve the phase estimate. Able-bodied bypass adapter experiments demonstrate that the phase variable controller replicates normative able-bodied kinematic trajectories with a root mean squared error of 12.66° and 2.64° for the knee and ankle, respectively. The knee and ankle joints provided on average $0.39\,\mathrm{J/kg}$ and $0.21\,\mathrm{J/kg}$ per stride, compared to the normative averages of $0.34\,\mathrm{J/kg}$ and $0.21\,\mathrm{J/kg}$, respectively. Thus, this controller allows powered knee-ankle prostheses to perform net positive mechanical work to assist stair ascent.**

I. Introduction

Many activities of daily living, including stair and ramp ascent, require net positive work from the lower-limb joints. During stair ascent, the knee and ankle produce $0.34\,\mathrm{J/kg}$ and $0.21\,\mathrm{J/kg}$, respectively, to raise the user's center of mass to the next step [1]–[3]. Passive and semi-passive devices used by individuals with above-knee amputation cannot do net positive work, requiring the user to adopt compensatory behaviors [4]. In particular, the step-to ascent gait is characterized by a person climbing only one stair per gait cycle instead of two stairs as seen in standard step-over ascent. Step-to ascent puts more strain on the upper body and sound leg in order to clear the step and support body weight [5]. These behaviors can cause secondary conditions such as chronic back pain and arthritis in the sound leg [6], [7], making the step-to ascent strategy undesirable.

Powered prosthetic devices may be able to produce stair ascent gaits that are more biomechanically similar to able-bodied gait [8]–[13]. However, many of these studies have utilized predetermined trajectories or set-points to accomplish these tasks, obfuscating the user's control over the prosthesis and relying on time-consuming manual tuning of many control parameters for each participant. Volitional control methods, on the other hand, adapt joint trajectories to the user's movements or intent. Previous work utilizing myoelectric control based on electromyogram readings from the residual thigh allowed for control of the prosthetic knee during stance, but struggled with control during swing to achieve proper foot placement on the following stair step [14]. Another volitional control scheme uses a heuristic approach with a stance controller based on the torque-angle relationship with the residual thigh and a swing controller based on residual thigh motion [13], allowing for adaptation between level-ground walking and stair ascent. However, the swing controller is dependent on thigh angle, velocity, and acceleration, which may be susceptible to noise and less predictable than dependence on thigh angle alone.

Other indirect volitional controllers, such as those utilized in [15]–[17], use a phase variable to measure the user's progression through the gait cycle. The controllers command desired knee and ankle kinematics by creating a time-invariant relationship with the monotonic phase-variable, mapping values of phase to ankle and knee joint positions. The phase variable in these studies was defined by a global thigh angle. These works utilized this approach for both level-ground and incline walking, demonstrating intuitive control and reduction in the number of controller parameters and the resulting tuning time.

This paper extends the phase-variable control method to stair ascent, providing the user direct control over stepping progression through their residual thigh angle. We introduce two innovations over prior phase-based controllers to enable stair climbing. First, our controller defines the gait cycle to start at maximum hip flexion (MHF) instead of heel-strike (HS) in order to mitigate saturation of the phase variable. Phase saturation is caused by the previous assumption that both MHF and heelstrike occur simultaneously, which is not the case with stair ascent. Recent work by [18] has shown that similar saturation occurs during slow walking speeds and was dealt with by shifting phase to fit a sinusoidal profile matching the gait progression of the user. With stair ascent, saturation happens consistently at all speeds due to thigh kinematic behavior. The second innovation of this controller improves user synchronization by reparameterizing the desired joint patterns based on the average thigh trajectory, accounting for the nonlinearities observed during stair ascent. This controller is able to generate the net positive work at the knee and ankle required to achieve step-over stair ascent.

This work was supported by the National Institute of Child Health & Human Development of the NIH under Award Number R01HD094772 and by the National Science Foundation under Award Number 2024237. The content is solely the responsibility of the authors and does not necessarily represent the official views of the NIH or NSF.

Ross J. Cortino, Edgar Bolívar-Nieto, T. Kevin Best, and Robert D. Gregg are with the Department of Electrical Engineering and Computer Science and the Robotics Institute, University of Michigan, Ann Arbor, MI 48109. Contact: {cortinrj, ebolivar, tkbest, rdgregg}@umich.edu

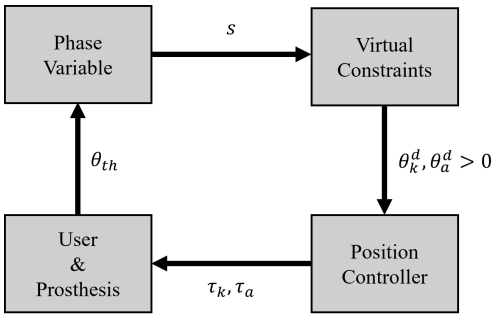

Fig. 1. A block diagram of the proposed control architecture. The phase estimate feeds into our virtual constraints outputting a desired knee and ankle angles, θ_k^{d} and θ_a^{d}. The position controller commands knee and ankle torques, τ_{k} and τ_{a}, which are utilized by scripts running on the prosthesis to produce knee and ankle kinematics. These changes in thigh and ankle angle allow the user to continue ascent resulting in changes in thigh trajectory, continuing the cycle.

II. Phase Variable Stair Ascent Controller

The stair ascent controller consists of three steps, shown in Fig. 1. First, the controller estimates the user's progression (i.e., phase) within the gait cycle from the global angle of the residual thigh, θ_{th}. Then, the controller calculates reference joint angles using a continuous representation of the knee and ankle kinematics parameterized by the gait phase, known as *Virtual Constraints*. Finally, low-level position controllers for each joint enforce the reference joint angles. The following sections discuss each step in detail.

A. Phase Variable

1) Background: Previous phase variable implementations for walking have represented the progression in the gait cycle as a monotonically increasing value between 0 and 1, with the gait cycle beginning and ending at heel strike. This was possible due to the thigh angle for level ground and incline walking having two roughly monotonic sections: one descending from the start of the gait cycle to the point of maximum hip extension (MHE) and the second ascending until HS. MHF and HS occur almost simultaneously during level ground walking. In [16], the phase variable, s, for walking was defined as

$$s = \begin{cases} \frac{\theta_{\mathrm{th}}^0 - \theta_{\mathrm{th}}}{\theta_{\mathrm{th}}^0 - \theta_{\mathrm{th}}^{\min}} \cdot c & \text{for } \theta_{\mathrm{th}} \text{ descending,} \\ 1 + \frac{1 - s_{\mathrm{m}}}{\theta_{\mathrm{th}}^0 - \theta_{\mathrm{th}}^{\mathrm{m}}} (\theta_{\mathrm{th}} - \theta_{\mathrm{th}}^0) & \text{for } \theta_{\mathrm{th}} \text{ ascending,} \end{cases} \quad (1)$$

where θ_{th}^0 represents the initial thigh angle at HS, $\theta_{\mathrm{th}}^{\min}$ represents the *ideal* thigh angle at MHE, and c represents the normalized time at which MHE occurs in a gait cycle [16], [17]. $\theta_{\mathrm{th}}^{\mathrm{m}}$ and s_{m} respectively represent the thigh and phase variable values at the *detected* point of MHE. These terms maintain continuity in phase when transitioning between descending and ascending definitions in the phase variable, in the event of a stride where the thigh at MHE is not equivalent to the ideal $\theta_{\mathrm{th}}^{\min}$. A finite state machine (FSM) was used to track if the user was on the ascending or descending portion of the thigh trajectory, detailed in [16].

This definition allowed for a reasonably linear approximation of phase in level-ground and incline walking because MHF occurs roughly at the end of the gait cycle. The thigh kinematics during stair ascent, however, do not exhibit this same behavior. Instead, MHF occurs earlier in the gait cycle followed by a third decreasing, roughly monotonic section until HS (see Fig. 2). This change in behavior compared to level ground and incline walking is a result of raising the leg over the next stair to clear the step in swing and then bringing it down for heel strike. Due to this difference in kinematics, θ_{th}^0 at HS no longer approximates the maximum thigh position, resulting in saturation of the phase variable in stair ascent (Fig. 2).

Phase saturation is undesirable because it leads to sections of the gait cycle where thigh angle no longer affects the positions of the knee and ankle, causing them to hold position for the remainder of the gait cycle. The effects of this saturation on the commanded joint trajectories can be seen in the right-most plot of Fig. 2.

2) Stair Ascent: To accommodate the difference in thigh kinematics between stair ascent and level ground walking, we have modified our definition of the gait cycle to begin at MHF instead of HS. This change in the definition of the gait cycle effectively shifts the thigh angle trajectory such that it has only two roughly monotonic sections, descending until MHE and ascending until MHF. The phase variable, s, can then be calculated using a modified form of (1), where the thigh angle at MHF, $\theta_{\mathrm{th}}^{\mathrm{MHF}}$, replaces θ_{th}^0:

$$s = \begin{cases} \frac{\theta_{\mathrm{th}}^{\mathrm{MHF}} - \theta_{\mathrm{th}}}{\theta_{\mathrm{th}}^{\mathrm{MHF}} - \theta_{\mathrm{th}}^{\min}} \cdot c & \text{for } \theta_{\mathrm{th}} \text{ descending,} \\ 1 + \frac{1 - s_{\mathrm{m}}}{\theta_{\mathrm{th}}^{\mathrm{MHF}} - \theta_{\mathrm{th}}^{\mathrm{m}}} (\theta_{\mathrm{th}} - \theta_{\mathrm{th}}^{\mathrm{MHF}}) & \text{for } \theta_{\mathrm{th}} \text{ ascending.} \end{cases} \quad (2)$$

In addition, modifications to the FSM controlling the transitions between the ascending and descending equations were required. The updated state definitions and their transition criteria are shown in Fig. 3. States S1 and S2 of the FSM correspond to the descending definition of s while S3 and S4 correspond to the ascending definition. The latter part of S1 and all of S2 and S3 are part of the stance phase of the gait cycle, while S4 and the beginning of S1 capture the swing phase. This is denoted within the FSM as FC $= 1$, with FC being a binary signal for foot contact. Successful MHF detection is denoted as MHF $= 1$, where real-time detection of MHF uses algorithms discussed in [19]. Our definition in (3) and the FSM reduce saturation of the phase variable. Fig. 2 illustrates our phase calculations and the resulting improvement in the predicted knee trajectory compared to [16]. Note that the non-linear phase trajectory results in phase shifting of the predicted knee trajectory with respect to the reference, which we will address in the next section.

B. Virtual Constraints

A Fourier series was used to represent the average able-bodied knee and ankle kinematics as functions of gait phase, termed the virtual constraints. Fourier series are useful for representing walking joint trajectories because they are periodic by nature and the smoothness of the trajectory can be

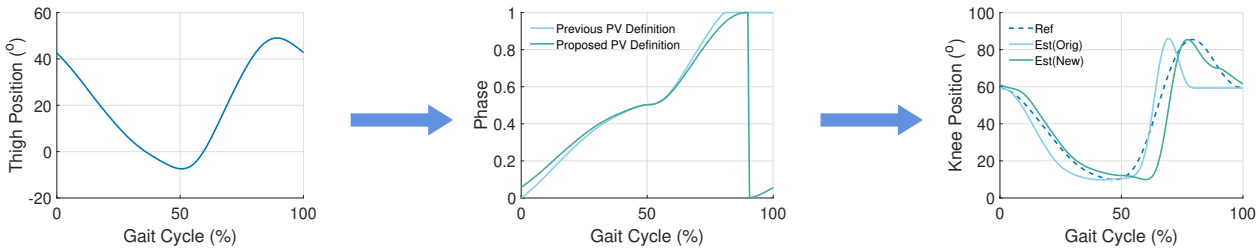

Fig. 2. Plots of average reference thigh angle for a stair incline of 30 degrees, comparison of current and proposed phase variable calculation trajectories, and resulting virtual constraint based knee joint kinematics. The proposed phase variable definition does not show the same saturation seen in the previous definition. This lack of saturation and monotonic behavior improves the estimated joint kinematics fit to the reference data.

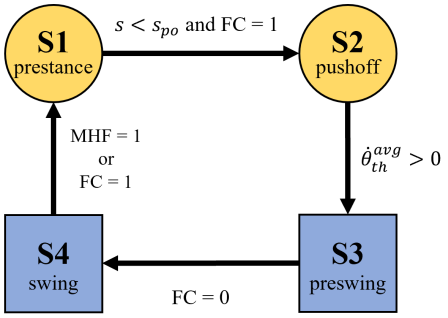

Fig. 3. Stair ascent state machine. The yellow circles correspond to the descending phase variable definition, while the blue squares correspond to the descending definition. S1 begins in swing after MHF has occurred and continues into stance until the onset of push-off onset where it then transitions to S2. S2 continues from push-off onset to the point of MHE where the average thigh velocity over a 40 ms window becomes positive, transitioning to S3. The state machine stays in S3 until FC $= 0$, where it then transitions to S4. Phase cannot decrease in S3 or S4. S4 continues until MHF $= 1$ and then transitions back to S1.

controlled through the order of the series [15]. Each desired joint angle $\theta_i^{\mathrm{d}}(s)$, $i \in \{\mathrm{k}, \mathrm{a}\}$, was determined by

$$\theta_i^{\mathrm{d}}(s) = \frac{1}{2}\rho_0 + \frac{1}{2}\rho_{\frac{N}{2}}\cos(\pi N s) + \sum_{j=1}^{N/2-1}\left[\rho_j \cos(\Omega_j s) - \psi_j \sin(\Omega_j s)\right], \tag{3}$$

where s denotes the phase variable, ρ_j and ψ_j are respectively the real and imaginary Fourier coefficients of the averaged able-bodied joint trajectories, $\Omega_j = 2\pi j$, and $N = 14$ is a finite number of samples with $N/2$ being the order of the Fourier series (chosen as a compromise between smoothness and RMSE with respect to the reference trajectories). A discrete Fourier transform (DFT) was used to determine the Fourier coefficients in a manner similar to [15] with an important modification described below.

The averaged able-bodied joint trajectories were calculated using the stair ascent data in [1], which reports joint kinematics per stride using normalized time. We interpolated these kinematics as functions of the average phase variable, based on the average thigh kinematics from the dataset. This accounts for non-linearities in the average phase trajectory, improving the phase synchronization (and thus the fit) of the estimated joint kinematics to the reference able-bodied

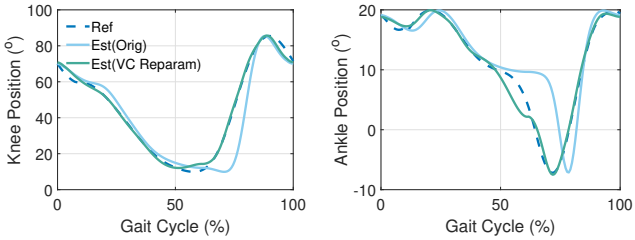

(a) (b)

Fig. 4. Plots of (a) knee and (b) ankle virtual constraint kinematics show improved estimation of able-bodied reference kinematics (Ref) with re-parameterized virtual constraints (Est(VC Reparam)) over virtual constraints without re-parameterization (Est(Orig)).

trajectory on average. Fig. 4a shows better estimation of the knee reference during early and middle swing which ensures clearing of the next step. Fig. 4b shows improved estimation of the ankle reference during maximum plantarflexion and early swing, which is important for powered push-off and step clearance. The interpolated reference knee and ankle trajectories were input to the DFT to calculate the coefficients of the Fourier functions [15]. Fig. 4 shows the calculated virtual constraints as functions of normalized time with and without re-parameterization.

C. Low-Level Position Control

The commanded joint torques at the knee, τ_{k}, and ankle, τ_{a}, were functions of the respective joint desired position ($\theta_{\mathrm{k}}^{\mathrm{d}}$ or $\theta_{\mathrm{a}}^{\mathrm{d}}$) by

$$\tau_i = k_{\mathrm{p}}^i(\theta_i^{\mathrm{d}} - \theta_i) + k_{\mathrm{i}}^i \int \left(\theta_i^{\mathrm{d}} - \theta_i\right) dt - k_{\mathrm{d}}^i \dot{\theta}_i, \tag{4}$$

where k_{p}^i, k_{i}^i, and k_{d}^i are proportional, integral, and derivative gains for the both knee and ankle joints. Terms for the desired joint velocities were neglected in order to limit vibrations that naturally arose due to the prosthesis's minimal inherent viscous losses [20].

III. Experimental Results

A. Methods

The proposed control method was implemented on the powered knee-ankle prosthesis designed in [20], shown in Fig. 5. This prosthesis features high torque, low impedance actuators (ILM 85 $\times$ 26 motor kit, RoboDrive, Seefeld,

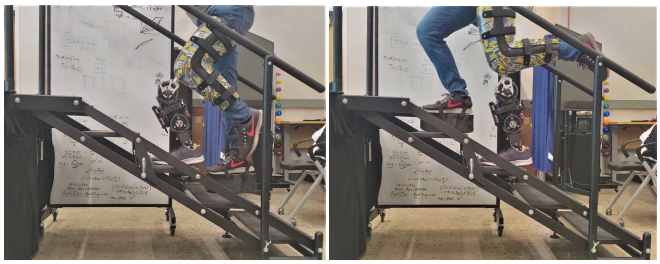

(a) (b)

Fig. 5. Photo of the able-bodied participant using the prosthesis for stair ascent during the experiments. The participant and configuration of the prosthesis are shown at (a) the beginning of stance and (b) at push-off. A shoe lift was worn on the contralateral foot in order to equalize leg lengths.

Germany) with custom 22:1 single-stage stepped-planet compound planetary gear transmissions. The motors are driven by G-SOLO Twitter R80A/80VDC drives (Elmo Motion Control, Petah Tikva, Israel). A prosthetic foot (Ottobock Lo Rider, 1E57) is mounted below a 6-axis load cell (Sunrise Instruments, Nanning, China), which mounts to the distal end of the ankle joint. The control and signal processing code is implemented on a myRIO 1900 (National Instruments, Austin, TX) mounted on the front of the prosthesis. All control code is executed at 500 Hz. Four on-board LiPo batteries (TP870-3SR70, Thunder Power, Las Vegas, NV) connected in series power the prosthesis. The global orientation of the residual thigh is measured using a 3DM-CX5-25 IMU (LORD Microstrain, Williston, VT) affixed to the proximal end of the knee actuator. Motor positions are measured by E5, 3600 cpr optical quadrature encoders (US Digital, Vancouver, WA). Joint velocities are estimated using second-order Savitzky-Golay differentiation.

This prosthesis was used because it has sufficiently powerful actuators to enable accurate position tracking during power intensive tasks, such as stair ascent. To demonstrate the merit of the control strategy, an experienced able-bodied user was fit with the prosthesis using a leg bypass adapter. The study was approved by the University of Michigan Review Board (HUM00166976) and the participant wore a safety harness at all times. In each trial, the participant walked up a dual handrail staircase with five steps inclined at 30 degrees (see Fig. 5). The specific stair inclination was chosen based on OSHA and other work place standards for stair inclination [21]. Before data collection, the position gains, $\theta_{\text{th}}^{\text{MHF}}$, $\theta_{\text{th}}^{\text{min}}$, and phase variable constant c were tuned while the participant ascended the staircase. To avoid fatigue during data collection, trials were performed over 3 separate testing periods, with 10 trials per period. This resulted in 30 full steady-state strides with the prosthesis (taking the middle stride of each trial as steady state). Kinetic and kinematic data were recorded from the prosthesis. A video of an example trial is available in the supplementary material.

B. Results

The joint kinematics and phase variable from the 30 trials were averaged and plotted against normative able-bodied trajectories in Fig. 6. Fig. 7 shows the average joint power and moments. Both figures use our gait cycle definition in Sec. II-A.2, *i.e.*, the gait cycle begins and ends at MHF. The normative able-bodied joint kinematics and kinetics correspond to [1] and [2], respectively.

The average phase trajectory (Fig. 6a) was monotonic and approximately reached one at the end of the gait cycle. It was relatively linear with no observed saturation of the phase variable at the end of the gait cycle. The average knee trajectory matched the reference able-bodied knee trajectory in Fig. 6b with a root mean squared error (RMSE) of $12.66°$. The difference between them was greatest in early swing. Similarly, this segment of the gait cycle had a large standard deviation of actual knee position, which matched the variability in the phase variable. The average ankle trajectory matched the able-bodied reference trajectory in Fig. 6c with an RMSE of $2.64°$. For the majority of the gait cycle, the mean ankle joint position was within a standard deviation of the reference. The largest standard deviations in position were found in the same region of the gait cycle as with the knee kinematics and phase variable. The largest standard deviation of the able-bodied data appeared in early swing.

The average knee torque (Fig. 7a) matched the able-bodied knee torque for the majority of the gait cycle (RMSE: 20.60 N·m). The peak torque of the measured data was greater than the able-bodied reference. Larger torques were applied over a longer period of time when compared to the reference, which may be an artifact of the additional limb mass and leg length from the bypass adapter. The average commanded ankle torque, Fig. 7b, matched the able-bodied ankle torque during the first half of the gait cycle (RMSE: 33.86 N·m). The peak ankle torque commanded during this period was greater than that of the able-bodied. Sec. IV-B discusses the differences between able-bodied and commanded torques.

The average knee power in Fig. 7c exhibited a similar peak and general pattern to the able-bodied data (RMSE: 34.14 W). However, the peak occurred slightly later and over a shorter interval in the gait cycle compared to the reference. The commanded power closely matched the reference during swing. The average ankle power in Fig. 7d followed the general trend of the able-bodied power data as well (RMSE: 38.14 W). Ankle power was greater than able-bodied for the first 50% of the gait cycle. The second half of the gait cycle exhibited ankle power that is characteristic of push-off, but was less than the able-bodied reference. See Sec. IV-B for the corresponding discussion. Despite these differences between the actual and reference joint power, we find that the knee and ankle joints provided on average $0.39\,\text{J/kg}$ and $0.21\,\text{J/kg}$ per stride, closely matching the normative averages of $0.34\,\text{J/kg}$ and $0.21\,\text{J/kg}$, respectively.

IV. Discussion

A. Advantages of the Control Strategy

A problem noted in previous phase-variable control strategies [15], [16] was that saturation can occur when $\theta_{\text{th}}^{\text{MHF}}$ is greater than θ_{th}^{0}. By utilizing real-time MHF detection

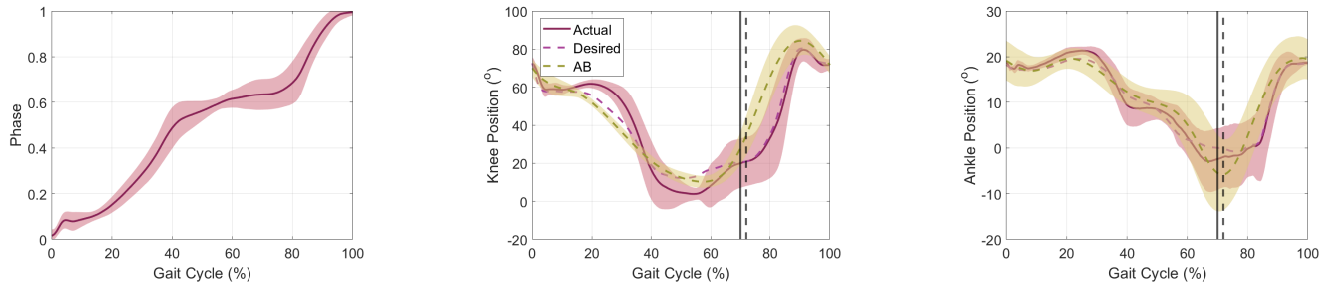

Fig. 6. Plots of (a) phase variable (b) knee kinematics and (c) ankle kinematics averaged over all 30 experimental strides. The able-bodied reference trajectory for each joint is denoted as AB, while the commanded and true position of each joint are denoted as Desired and Actual, respectively The relative linearity of the phase variable combined with the well-fitting virtual constraints produced joint kinematics resembling able-bodied stair ascent gait. The vertical black lines denote when toe-off occurs within the gait cycle, dashed representing able-bodied and solid representing when toe-off occurred for the participant. Positive knee and ankle angles denote knee flexion and ankle dorsiflexion, respectively.

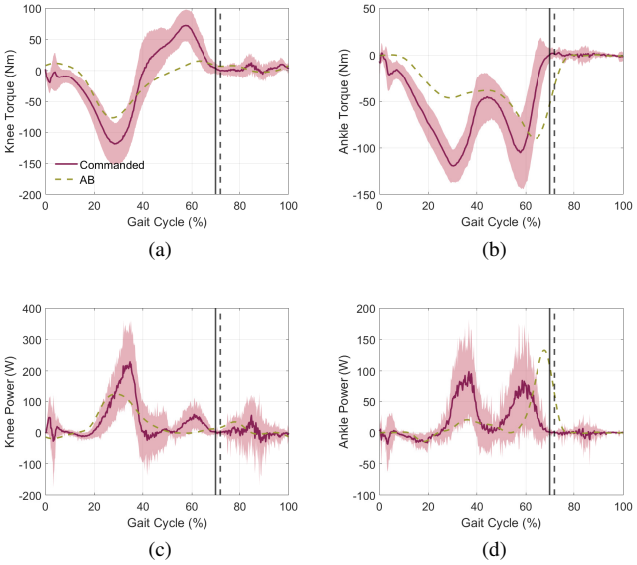

Fig. 7. Plots of (a) knee torque, (b) ankle torque, (c) knee power, and (d) ankle power averaged over all 30 experimental strides. The joint kinetics resembling able-bodied stair ascent gait kinetics with the exception of a lack of push-off at the ankle. Positive knee and ankle torques denote knee flexion and ankle dorsiflexion, respectively.

and a shifted gait cycle definition, we were able to reduce saturation of the phase variable and produce an average phase variable that is mostly monotonic from start to end of the stride, as shown in Fig. 6. This result suggests that using a similar strategy for level-ground walking (as in [18]), ramp ascent/descent, and other activities may be beneficial.

Our virtual constraints, designed from normative joint trajectories for a stair inclination of 30°, allowed stair ascent for an able-bodied user of the powered knee-ankle prosthesis. During swing, we see the most similarity between actual and reference kinematics (Fig. 6), which is important for clearing the following step and achieving proper foot placement for the next stride. This allows for step-over stair ascent without tripping or toe-stubbing.

B. Limitations of Control Strategy and Study

While transitioning at MHF enables our phase variable approach, real-time MHF detection can be prone to false or premature detection. Premature detection of MHF can be problematic, as it can cause discontinuous changes in the phase variable and the resulting virtual constraints. Joint angle thresholds for MHF detection that adapt with the user's thigh position during ascent could be beneficial to prevent false detection. The current thresholds for MHF detection are based on the reference kinematics of a 30° incline. Improving robustness of MHF detection would also allow for a more robust FSM that enables non-standard gait progressions such as adjusting foot placement after MHF.

Further, the greatest deviations in the ankle and knee kinematic trajectories relative to the able-bodied references occured during toe-off and early swing. Fig. 6a shows the phase variable at this point in the gait cycle increased slower than the ideal linear phase. The supplemental video shows that, at this point, the participant's thigh did not move forward as expected, instead moving slightly backwards after toe-off before forward movement begins to clear the next step. The participant noted this movement was involuntary and appeared to be related to balance after loss of foot contact. At this point in the gait cycle, phase is not allowed to decrease, resulting in the pausing behavior between 60-80% in Fig. 6a. Fig. 7 shows that push-off torque at the ankle occurred earlier in the gait cycle compared to the able-bodied reference. Similarly toe-off occurred earlier than the able-bodied reference. Push-off is important for propelling the user into swing, and may have an effect on user balance in terminal stance. Utilizing a feed-forward approach to calculating phase at this point in the gait cycle (as in [22]) could be a potential solution to avoiding the phase variable pause associated with MHE. This would improve push-off and toe-off timing by ensuring the calculated virtual constraints match the able-bodied references.

This study was also limited by the enrollment of an able-bodied participant using a bypass adapter. It is possible that the unexpected decrease of the thigh angle in early swing, as well as the premature toe-off, could be a result of the mechanics of bypass adapter walking. In particular, walking may be asymmetric because the knee joint centers are not the same between the sound leg (wearing a foot lift) and the prosthetic leg worn with a bypass. Further studies with

amputee participants are necessary to address this limitation.

Finally, the FSM in the proposed controller only allowed sequential state progression, so phase could not decrease in terminal stance and swing. In future studies, we will develop a more versatile FSM that allows for switching between stance and swing without the need to progress through the entire gait cycle (as done in [16] for level-ground walking). This would be beneficial if a user needs to adjust their foot placement after MHF or bring their leg back down to the stair after just pushing off.

C. Extension of Control Strategy for Stair Descent

Future work will apply a similar control strategy to stair descent. While the general premise will be the same as the ascent controller, special consideration needs to be given to the small thigh range of motion relative to the knee and ankle ranges of motion during descent. Because of this difference in range of motion, the effective gain applied by the virtual constraints when mapping thigh angle to the knee or ankle angles will be quite high. This is especially problematic at the knee, which can influence thigh motion and create unstable feedback interactions, particularly during swing.

V. Conclusion

In this paper, we introduced a new indirect volitional control approach for stair ascent based on a phase variable. A novel phase variable was presented based on the user's thigh angle where the gait cycle was defined to start at MHF. Real-time detection of MHF and FC allowed a finite state machine to control the transitions between definitions of the phase variable within the gait cycle. The new phase variable definition, combined with virtual constraints derived from able-bodied stair kinematics, allowed the user to ascend stairs in a normative, step-over gait. Experiments with an able-bodied participant wearing a bypass adapter validated our control approach. The supplemental video showcases that the proposed controller allowed the able-bodied participant to accomplish stair-over ascent over multiple strides.

Future work will include similar experiments with participants with an above-knee amputation. An extension of this control approach would allow for adaptation to stair height instead of assuming stair height matches an incline of 30°. A similar control scheme to the one proposed could also be employed for powered stair descent. Another extension of this controller would be its implementation with a higher level classifier as shown in [19] in order to enable continuous locomotion between tasks. All of these future applications will prove important to better understanding this controller's capabilities, benefits, and shortcomings.

References

[1] E. Reznick, K. Embry, R. Neuman, E. Bolívar-Nieto, N. Fey, and R. Gregg, "Human lower-limb kinematics and kinetics during continuously varying locomotion," *Scientific Data*, pp. 1–15, 2021.

[2] R. Riener, M. Rabuffetti, and C. Frigo, "Stair ascent and descent at different inclinations," *Gait Posture*, vol. 15, pp. 32–44, 2002.

[3] J. Camargo, A. Ramanathan, W. Flanagan, and A. Young, "A comprehensive, open-source dataset of lower limb biomechanics in multiple conditions of stairs, ramps, and level-ground ambulation and transitions," *J. Biomechanics*, vol. 119, p. 110320, 2021.

[4] H. Hobara, Y. Kobayashi, T. Nakamura, N. Yamasaki, K. Nakazawa, M. Akai, and T. Ogata, "Lower extremity joint kinematics of stair ascent in transfemoral amputees," *Prosthetics and Orthotics International*, vol. 35, no. 4, pp. 467–472, 2011.

[5] D. J. Lura, M. W. Wernke, S. L. Carey, J. T. Kahle, R. M. Miro, and M. J. Highsmith, "Crossover study of amputee stair ascent and descent biomechanics using Genium and C-Leg prostheses with comparison to non-amputee control," *Gait Posture*, vol. 58, pp. 103–107, 2017.

[6] D. M. Ehde, D. G. Smith, J. M. Czerniecki, K. M. Campbell, D. M. Malchow, and L. R. Robinson, "Back pain as a secondary disability in persons with lower limb amputations," *Arch. Phys. Med. Rehabil.*, vol. 82, no. 6, pp. 731–734, 2001.

[7] D. C. Norvell, J. M. Czerniecki, G. E. Reiber, C. Maynard, J. A. Pecoraro, and N. S. Weiss, "The prevalence of knee pain and symptomatic knee osteoarthritis among veteran traumatic amputees and nonamputees," *Arch. Phys. Med. Rehabil.*, vol. 86, no. 3, pp. 487–493, 2005.

[8] M. Tran, L. Gabert, M. Cempini, and T. Lenzi, "A Lightweight, Efficient Fully Powered Knee Prosthesis with Actively Variable Transmission," *IEEE Robotics and Automation Letters*, vol. 4, no. 2, pp. 1186–1193, 2019.

[9] T. Lenzi, M. Cempini, L. Hargrove, and T. Kuiken, "Design, development, and testing of a lightweight hybrid robotic knee prosthesis," *Int. J. Robotics Research*, vol. 37, no. 8, pp. 953–976, 2018.

[10] S. Culver, H. Bartlett, A. Shultz, and M. Goldfarb, "A stair ascent and descent controller for a powered ankle prosthesis," *IEEE Trans. Neural Syst. Rehabilitation Eng.*, vol. 26, no. 5, pp. 993–1002, 2018.

[11] A. M. Simon, K. A. Ingraham, N. P. Fey, S. B. Finucane, R. D. Lipschutz, A. J. Young, and L. J. Hargrove, "Configuring a powered knee and ankle prosthesis for transfemoral amputees within five specific ambulation modes," *PLoS ONE*, vol. 9, no. 6, 2014.

[12] E. D. Ledoux and M. Goldfarb, "Control and evaluation of a powered transfemoral prosthesis for stair ascent," *IEEE Trans. Neural Syst. Rehabilitation Eng.*, vol. 25, no. 7, pp. 917–924, 2017.

[13] S. Hood, L. Gabert, and T. Lenzi, "Powered knee and ankle prosthesis with adaptive control enables climbing stairs with different stair heights, cadences, and gait patterns," *TechRxiv*, no. 1925343, pp. 1–11, 2020.

[14] C. D. Hoover, G. D. Fulk, and K. B. Fite, "Stair ascent with a powered transfemoral prosthesis under direct myoelectric control," *IEEE/ASME Trans. Mechatronics*, vol. 18, no. 3, pp. 1191–1200, 2013.

[15] D. Quintero, D. J. Villarreal, D. J. Lambert, S. Kapp, and R. D. Gregg, "Continuous-phase control of a powered knee-ankle prosthesis: Amputee experiments across speeds and inclines," *IEEE Trans. Robotics*, vol. 34, no. 3, pp. 686–701, 2018.

[16] S. Rezazadeh, D. Quintero, N. Divekar, E. Reznick, L. Gray, and R. D. Gregg, "A phase variable approach for improved rhythmic and non-rhythmic control of a powered knee-ankle prosthesis," *IEEE Access*, vol. 7, pp. 109 840–109 855, 2019.

[17] T. K. Best, K. R. Embry, E. J. Rouse, and R. D. Gregg, "Phase-Variable Control of a Powered Knee-Ankle Prosthesis over Continuously Varying Speeds and Inclines," *IEEE Int. Conf. Intell. Robots Syst.*, 2021.

[18] W. Hong, N. Anil Kumar, and P. Hur, "A phase-shifting based human gait phase estimation for powered transfemoral prostheses," *IEEE Robotics and Automation Letters*, vol. 6, no. 3, pp. 5113–5120, 2021.

[19] S. Cheng, E. Bolivar-Nieto, and R. D. Gregg, "Real-time activity recognition with instantaneous characteristic features of thigh kinematics," *IEEE Trans. Neural Syst. Rehabilitation Eng.*, pp. 1–1, 2021.

[20] T. Elery, S. Rezazadeh, C. Nesler, and R. D. Gregg, "Design and Validation of a Powered Knee-Ankle Prosthesis With High-Torque, Low-Impedance Actuators," *IEEE Trans. Robot.*, pp. 1–20, 2020.

[21] *Stairways*, OSHA Standard 1910.25, 2019.

[22] T. Best, C. Welker, E. Rouse, and R. Gregg, "Phase-based impedance control of a powered knee-ankle prosthesis for tuning-free locomotion over speeds and inclines," *TechRvix*, 2022.

[23] E. J. Wolf, V. Q. Everding, A. L. Linberg, B. L. Schnall, J. M. Czerniecki, and J. M. Gambel, "Assessment of transfemoral amputees using C-Leg and Power Knee for ascending and descending inclines and steps," *J. Rehabil. Res. Dev.*, vol. 49, no. 6, p. 831, 2012.

[24] B. E. Lawson, H. A. Varol, A. Huff, E. Erdemir, and M. Goldfarb, "Control of stair ascent and descent with a powered transfemoral prosthesis," *IEEE Trans. Neural Syst. Rehabilitation Eng.*, vol. 21, no. 3, pp. 466–473, 2013.